Plasma-polymerized multistacked bipolar gate dielectric for organic thin-film transistors

Woo-Jun Yoon [a,1,3], Dhiman Bhattacharyya [b,2,3], Richard B. Timmons [b], Paul R. Berger [a,c,*]

[a] Department of Electrical and Computer Engineering, The Ohio State University, Columbus, OH 43210, USA
[b] Department of Chemistry and Biochemistry, University of Texas at Arlington, Arlington, TX 76019, USA
[c] Department of Physics, The Ohio State University, Columbus, OH 43210, USA

ARTICLE INFO

ABSTRACT

A 10-layer stack of bipolar gate dielectric was formed by sequential layer-by-layer deposition using pulsed radio frequency (RF) plasma polymerization of allylamine and vinyl acetic acid monomers. Due to polar groups localized at the interfaces between each consecutive layer by alternating amine ($-NH_2$) and carboxylic acid ($-COOH$) functional groups, a 60 nm thick multilayer structure demonstrated relatively high dielectric constant of 4.4 with extremely smooth and crack/pin-hole free surfaces. Without any post-deposition thermal annealing, a 10-layer stack of bipolar dielectric layers shows a low leakage current density ($\sim 1 \times 10^{-6}$ A/cm^2 at 2 MV/cm) with high breakdown fields (>4 MV/cm). With a 10-layer stack of bipolar gate dielectrics, low supply voltage regioregular poly-(3-hexythiophene) (P3HT) organic thin-film transistors (OTFT) were tested. P3HT OTFTs demonstrated low-voltage operation and moderate field-effect mobility up to $\sim 3.4 \times 10^{-3}$ cm^2/V s in the saturation region with the drain voltage a -12 V. The threshold voltage in the saturation region and on–off current ratio were measured to be $+1.4$ V and $\sim 1.2 \times 10^2$, respectively.

© 2010 Elsevier B.V. All rights reserved.

1. Introduction

Organic-based gate dielectrics with high dielectric constant (k) have made remarkable progress toward high performance and low-voltage operation organic thin-film transistors (OTFT) in the last two decades [1–8]. Among various gate dielectric deposition methods, plasma polymerization has gained increasing interest for its ability to develop new thin gate dielectrics toward electronic application due to simple processing, wide selection of monomers, and low deposition temperature [9,10]. For example, both high- and low-k dielectric have been successfully plasma-polymerized using different monomers [11–15]. More recently, high-k gate dielectrics deposited under plasma polymerization have been implemented in OTFTs, greatly reducing OTFT's operating voltages while exhibiting good device performances [11,12].

Pulsed RF plasma polymerization can be employed to alter systematically the density of the monomer functional groups through controlled variation of the plasma on/off duty cycle. As a result, functional groups present in the monomer can be retained significantly in the polymerized films [13,14]. Under pulsed plasma polymerization conditions, the k values of deposited films can be tailored by employing different polarizability of monomer functional groups. Recently, a 50 nm thick multilayer structure demonstrated relatively high dielectric constant of ~ 6 without employing any post-deposition thermal annealing, which was attributed to the presence of polar groups, specifically ammonium ($-NH_3^+$) and carboxylate ($-COO^-$) localized at the interfaces between each consecutive plasma deposited

layer [14]. It should be noted that carbon-based materials, like polyimides, generally exhibit a dielectric constant of only 2.0–2.5.

The significant advantage of multistacked bipolar films is that the leakage current can be effectively suppressed, while the film can be synthesized thin, typically less than 50 nm [14]. In our previous study, we found the leakage current is decreased two orders of magnitude even though the total thickness of film is decreased while increasing the number of multilayers in the stack, indicating the number of interfaces within each deposited film is an important factor to control the leakage current in multilayer stacked bipolar polymer films [14].

In this article, we report low-voltage operation regioregular poly-(3-hexylthiophene) (P3HT) OTFTs with pulsed RF plasma-polymerized multistacked bipolar gate dielectric.

2. Experimental

A carboxylic acid (–COOH) containing monomer, vinyl acetic acid (VAA), and an amine (–NH$_2$) containing monomer, allylamine (AA), were polymerized under pulsed RF plasma operational conditions. The monomers were used as-received without further purification. A polymeric thin film of AA was first deposited by pulsed RF plasma polymerization on the substrate which was then followed by the deposition of a thin film of VAA. The sequential layer-by-layer deposition of these films was performed to obtain a total 10-layer stacked structure of pulsed RF plasma-polymerized AA (PP-AA) and VAA (PP-VAA), containing polar groups localized at the interfaces between each consecutive layer. For pulsed plasma deposition of VAA, a plasma duty cycle of 2/30 (plasma on-time, ms/plasma off-time, ms) was used at a monomer pressure 160 mTorr and 150 W power input. Allylamine was plasma polymerized at a duty cycle of 10/30, monomer pressure 70 mTorr and 100 W power input. Substrate temperature was nominally held at room temperature. Further details of condition for pulsed RF plasma polymerization of VAA and AA can be found elsewhere [14]. The nominal total thicknesses and the refractive index of the deposited films were estimated to be ∼60 nm, corresponding to individual layers of ∼6 nm, and 1.61, respectively, as measured by single wavelength ellipsometry. The surface morphologies of a 10-layer stack of polymeric films were studied using a Dimension 3100 atomic force microscopy (AFM) (Veeco Instruments) in tapping mode.

For capacitance–voltage (C–V) characterization with an LCR meter (Agilent 4284A), the polymer films were deposited on p-type silicon wafers with a resistivity of 4.4 Ω cm for metal–insulator–semiconductor (MIS) capacitors. After deposition of 10-layer stack of PP-AA and PP-VAA, the MIS capacitors were completed by shadowmask electron beam evaporation (∼10^{-7} Torr) of a 100 nm thick Au gate metal, directly onto the multilayer stack surface. The final MIS structure fabricated was a p-Si/10-layer stack of PP-AA and PP-VAA/Au. The active area of each MIS capacitor studied was 0.283 mm^2. Leakage current density versus electric field characteristics ($J_{Leakage}$–E) of MIS capacitors were

measured with a semiconductor parameter analyzer (Agilent 4156) at room temperature under darkness. All MIS capacitors fabricated were tested without any post-deposition annealing.

A 10-layer stack of film as the gate dielectric was used for a bottom contact OTFTs. The Si substrates were processed using standard silicon degreasing and RCA cleaning procedures prior to plasma polymerization. A heavily doped n-type silicon substrate with a resistivity of 0.003 Ω cm was used as the gate. After deposition of multilayer stacks of thin films, the Au source and drain contacts are formed by standard photolithography and lift-off, defining a channel length of 7 μm and width of 135 μm. It was shown that the plasma-polymerized multistacked gate dielectrics are resistant to immersion in typical chemical solvents for standard photolithography and lift-off. They are robust enough to withstand conventional photolithographic processing with no observable film shrinkage, warping or peeling.

Thin films of the P3HT were then deposited by spin coating from a concentration of 8 mg/ml in chloroform in an inert glove box environment with ⩽1 ppm level of oxygen and moisture. The regioregular P3HT (Merck Chemicals Ltd.) with 94.5% regioregularity was used without further purification. The P3HT used here has a weight-average molecular weight (M_w) of 26,200 g/mol, corresponding to a number-average molecular weight (M_n) of 13,000 g/mol, and with a polydispersity (M_w/M_n) of ∼2. The P3HT OTFTs were kept in a vacuum at pressures below 10^{-6} Torr for 10 h to remove any unintended doping. Prior to the measurement, the completed P3HT OTFTs were briefly annealed at 110 °C for 10 min in N$_2$ atmosphere. Electrical characterizations of the P3HT OTFTs were performed with a semiconductor parameter analyzer (Agilent 4156) at room temperature under darkness in ambient air.

3. Results and discussion

The chemical structures of monomers used for plasma polymerization are shown in Fig. 1. Each AA and VAA monomer has the requisite monomer functionalities, –NH$_2$ and –COOH groups, respectively. Under pulsed plasma operational conditions, these functional groups in the monomer structure are retained significantly in the films. Explicit evidence for the presence of the –COO$^-$ and –NH$_3^+$ polar entities in the interface of the multilayer structure was provided using X-ray photoelectron spectroscopy and attenuated total reflectance Fourier transform-IR spectroscopy, described in detail elsewhere [14].

Fig. 2 shows the AFM tapping mode height images (1 μm × 1 μm) for a 10-layer stack of PP-AA and PP-VAA films deposited on a silicon substrate by pulsed RF plasma polymerization. The root-mean-square (RMS) roughness of the deposited film is ∼0.129 nm in the image Z range of 1.703 nm, demonstrating pulsed RF plasma polymerization could be very effective for producing extremely smooth surfaces. In addition, no crack/pin-holes were observed over different positions on the surface scanned by AFM.

Fig. 3a shows a typical C–V response of an MIS capacitor (p-Si/10-layer stack of alternating AA and VAA/Au) at
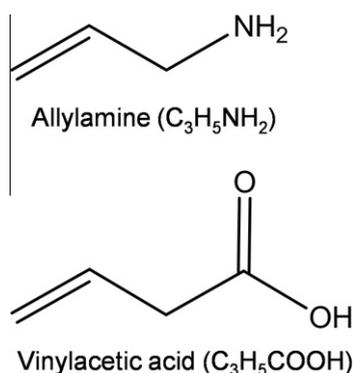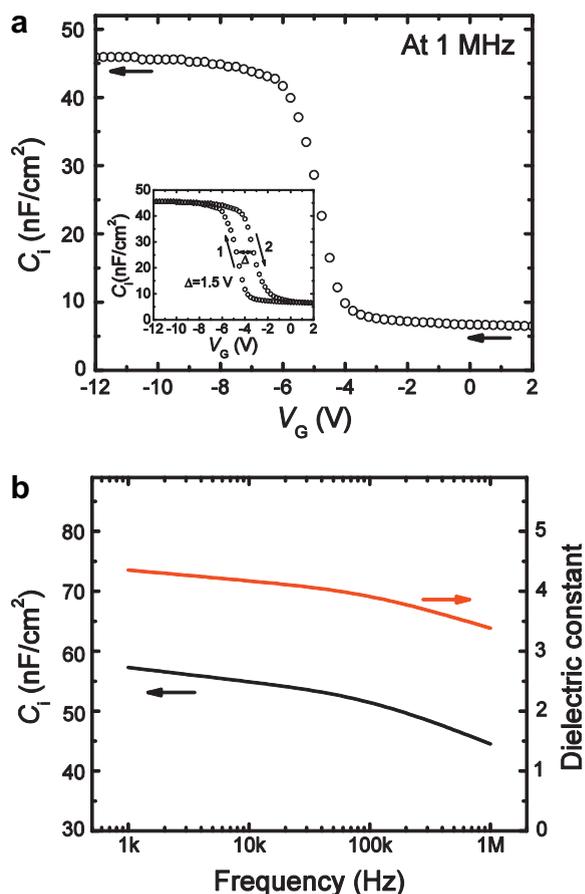
Fig. 1. Chemical structure of monomers used for polymerization under pulsed RF plasma condition: an amine (–NH₂) containing monomer, allylamine (C₃H₅NH₃), and a carboxylic acid (–COOH) containing monomer, vinyl acetic acid (CH₃COOH).
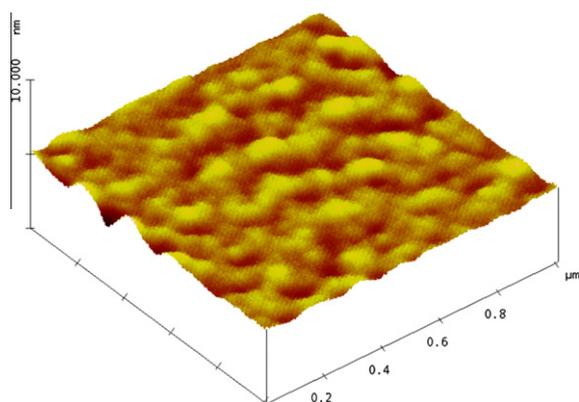
Fig. 2. AFM images (1 μm × 1 μm) for a 10-layer stack of gate dielectric layers deposited by pulsed RF plasma polymerization. The RMS roughness of the gate dielectric layers was 0.129 nm with the image Z range of 1.703 nm.

Fig. 3. (a) C–V characteristics of MIS capacitors at 1 MHz for a pulsed RF plasma-polymerized gate dielectric ($\sim$60 nm). The inset shows the hysteresis behavior of the MIS capacitor. (b) Frequency dependency of the gate capacitance per area (C_i) in accumulation and the dielectric constant. The dielectric constant extracted at 1 kHz is $\sim$4.4.

1 MHz frequency clearly showing depletion at positive gate voltage (V_G) and accumulation at negative V_G when the V_G was swept from +V_G to –V_G. It shows the shift to more negative values of V_G along the voltage axis of a C–V curves with respect to the ideal C–V curve due to uniformly distributed trapped charges during plasma polymerization process across the polymerized films thickness [15]. The inset of Fig. 3a shows the hysteresis behavior of the capacitor for a sweep of +V_G to –V_G and a return sweep –V_G to +V_G, which exhibits a $\sim$1.5 V voltage shift at 1 MHz. The voltage shift of the C–V curves could be attributed to positive mobile charges associated with the multilayered bipolar gate dielectric. For positive V_G, positive mobile ions drift to the insulator–semiconductor interface, giving a negative voltage shift. For large negative V_G, the positive mobile charges are attracted to the gate-insulator interface where it exhibits less influence upon the measured C–V curves. The total voltage shift, ΔV (V) is given as $\Delta V = -Q/C_i$ where Q is the effective net charge per unit area (cm^{-2}), and C_i is the measured gate capacitance per unit area (F/cm^2). The effective net charge density in the gate dielectric layer is estimated to be $\sim$4.4 $\times$ 10^{12} cm^{-2}. The

C_i tends to shift to slightly higher values when decreasing the frequency for all capacitors, as shown in Fig. 3b. An observed frequency dependent dispersion in the accumulation region can be attributed to the slow polarization of the gate dielectric at higher frequencies and this polarization can lead to an increase in the induced charge at lower frequencies [16]. The k values of the multilayer gate dielectric were calculated at four different frequencies using $k = C_i \cdot t/\varepsilon_0$, where ε_0 is the permittivity in vacuum, and t is the thickness. The calculated dielectric constant was 4.4 at 1 kHz (Fig. 3b). For the extraction of field-effect mobility values of P3HT OTFTs in the saturation region, the C_i equal to 57.3 nF/cm^2 at 1 kHz was considered.

Fig. 4 illustrates the leakage current density versus electric field, $J_{Leakage}$–E, for the 10-layer stack of gate dielectric. The leakage current density was 7.34 $\times$ 10^{-6} A/cm^2 at 2 MV/cm. The breakdown field was estimated to be larger than 4 MV/cm. The inset of Fig. 4 is the leakage current density versus the voltage ($J_{Leakage}$–V) characteristics for the MIS capacitors. It should be noted that all the multilayer gate dielectrics in this study were measured without any post-deposition annealing.
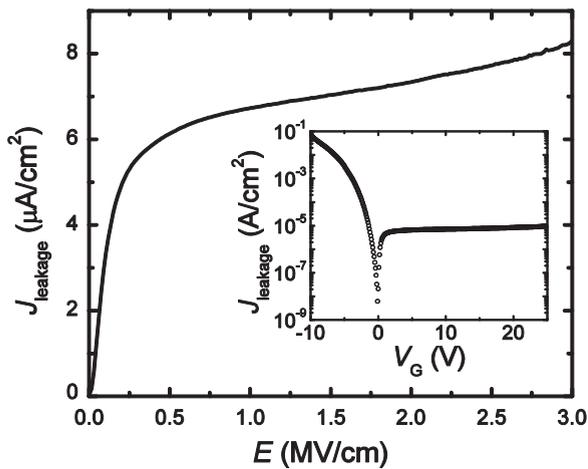
Fig. 4. $J_{Leakage}$–E characteristics of MIS capacitors. The breakdown field is estimated >4 MV/cm. The inset shows $J_{Leakage}$–V characteristics of the capacitors.

Fig. 5a shows the output characteristics for P3HT OTFTs with applied drain voltage (V_D) ranging from 0 to −15 V with V_G varying from 4 to −6 V. The devices operate at relatively low supply voltages. However, a large off-state I_D at the level of ~1 × 10^{-9} A at V_G = 0 was observed using fresh devices tested in air without any encapsulation immediately after completion of the fabrication process. Although a non-zero I_D could be reduced by applying a positive V_G, the I_D at V_G = 4 V was only one order of magnitude lower than that at V_G = 0 V. It has been known that an off-state I_D could increase over the extended exposure in ambient air due to the high bulk conductivity of P3HT attributed from unreduced P3HT and oxygen doping [17,18]. However, considering that the fresh devices were tested immediately after completion of fabrication, a high off-state I_D at a positive V_G could be due to doping to P3HT by oxygen from the surfaces of plasma-polymerized films since plasma-polymerized films have a strong affinity for oxygen and

moisture [19]. For the transfer characteristic in the saturation region at V_D = −10 V and V_D = −12 V, the plot of $I_D^{1/2}$ – V_G is shown in Fig. 5b. The mobility in the saturation region (μ_{sat}), and the threshold voltage (V_T) are calculated from

$$I_D = \frac{W}{2L}C_{total}\mu(V_G - V_T)^2 \tag{1}$$

At V_D = −12 V, the μ_{sat} and V_T are estimated to be 3.4 × 10^{-3} cm^2/V s and +1.4 V, respectively, while V_D = −10 V, the μ_{sat} and V_T are 2.9 × 10^{-3} cm^2/V s and +1.5 V, respectively. The devices showed a dependence of μ_{sat} on V_G (not shown here). Due to a large off-state I_D, an on–off current ratio ($I_{on/off}$) of only ~1.2 × 10^2 was measured. No significant variation of estimated μ_{sat}, V_T, and $I_{on/off}$ was recorded over more than 5 devices.

4. Conclusions

In conclusion, pulsed RF plasma polymerization could be very effective for producing extremely smooth and crack/pin-hole free gate dielectrics. It was shown that the plasma-polymerized multistacked gate dielectrics are robust enough to withstand conventional photolithographic processing with no observable film shrinkage, warping or peeling. Finally it was demonstrated that the P3HT OTFTs operate at low supply voltages due to high-k values of pulsed RF plasma-polymerized multistacked gate dielectrics, achieved without post-production annealing. Further work is required to reduce possible oxygen doping to P3HT from the surface of plasma-polymerized gate dielectrics through surface passivation.
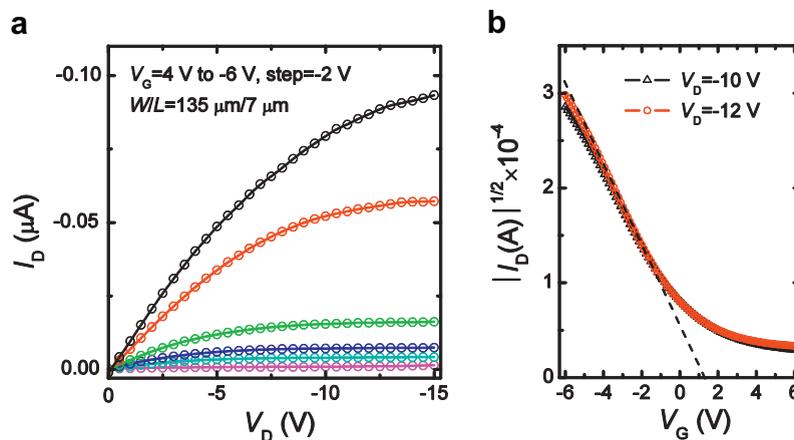
Acknowledgement

Fig. 5. (a) V_D–I_D characteristics of the P3HT OTFT with the applied V_D ranging from 0 to −15 V with V_G varying from 4 to −6 V in steps of −2 V. (b) $I_D^{1/2}$ – V_G characteristics of the P3HT OTFT with the V_G ranging from 6 to −6 V with V_D of −10 and −12 V.

References

[1] L.-L. Chua, P.K.H. Ho, H. Sirringhaus, R.H. Friend, Appl. Phys. Lett. 84 (2004) 3400.
[2] X. Peng, G. Horowitz, D. Fichou, F. Garnier, Appl. Phys. Lett. 57 (1990) 2013.
[3] Z. Bao, V. Kuck, J.A. Rogers, M.A. Paczkowski, Adv. Funct. Mater. 12 (2002) 526.
[4] Z. Bao, Y. Feng, A. Dodabalapur, V.R. Raju, A.J. Lovinger, Chem. Mater. 9 (1997) 1299.
[5] R. Parashkov, E. Becker, G. Ginev, T. Riedl, H.H. Johannes, W. Kowalsky, J. Appl. Phys. 95 (2004) 1594.
[6] I.M. Rutenberg, O.A. Scherman, R.H. Grubbs, W. Jiang, E. Garfunkel, Z. Bao, J. Am. Chem. Soc. 126 (2004) 4062.
[7] F.-C. Chen, C.-W. Chu, J. He, Y. Yang, J.-L. Lin, Appl. Phys. Lett. 85 (2004) 3295.
[8] Y.-Y. Noh, H. Sirringhaus, Org. Electron. 10 (2009) 174.
[9] H. Biederman (Ed.), Plasma Polymer Films, Imperial College Press, London, 2004.
[10] H. Biederman, Y. Osada, Plasma Polymerization Processes, Elsevier Science, 1992.
[11] Y. Xu, P.R. Berger, J. Cho, R.B. Timmons, J. Appl. Phys. 99 (2006) 014104.
[12] J.-S. Lim, P.-K. Shin, B.-J. Lee, S. Lee, Org. Electron. 11 (2010) 951.
[13] Y. Xu, P. Berger, J. Cho, R. Timmons, J. Electron. Mater. 33 (2004) 1240.
[14] D. Bhattacharyya, W.-J. Yoon, P.R. Berger, R.B. Timmons, Adv. Mater. 20 (2008) 2383.
[15] J.E. Klemberg-Sapieha, S. Sapieha, M.R. Wertheimer, A. Yelon, Appl. Phys. Lett. 37 (1980) 104.
[16] P.J. Brown, H. Sirringhus, M. Harrison, M. Shkunov, R.H. Friend, Phys. Rev. B 63 (2001) 1252041.
[17] M.S.A. Abdou, F.P. Orfino, Y. Son, S. Holdcroft, J. Am. Chem. Soc. 119 (1997) 4518.
[18] D.B.A. Rep, A.F. Morpurgo, T.M. Klapwijk, Org. Electron. 4 (2003) 201.
[19] H. Jiang, J.T. Grant, J. Enlow, W. Su, T.J. Bunning, J. Mater. Chem. 19 (2009) 2234.